eNeuro

Research Article: New Research | Cognition and Behavior

Chemogenetic silencing of prelimbic cortex to anterior dorsomedial striatum projection attenuates operant responding

https://doi.org/10.1523/ENEURO.0125-19.2019

Cite as: eNeuro 2019; 10.1523/ENEURO.0125-19.2019

Received: 31 March 2019
Revised: 28 August 2019
Accepted: 3 September 2019

Chemogenetic silencing of prelimbic cortex to anterior dorsomedial striatum projection attenuates operant responding

Abbreviated title: PL to aDMS silencing attenuates operant responding

Megan L. Shipman[1,2], Gregory C. Johnson[1,2], Mark E. Bouton[1], & John T. Green[1]

[1]University of Vermont Department of Psychological Science

[2]Neuroscience Graduate Program

MS, MB, and JG designed research, MS and GJ performed research, MS, GJ, and JG analyzed data, MS, JG, GJ, and MB wrote the paper

Correspondence should be addressed to:
John T. Green
Department of Psychological Science
2 Colchester Ave.
University of Vermont
Burlington, VT 05405
e-mail: john.green@uvm.edu

Number of figures: 5

Number of tables: 0

Number of multimedia: 0

Number of words for abstract: 255

Number of words for significance statement: 44

Number of words for introduction: 538

Number of words for discussion: 1643

Acknowledgements: We would like to thank David J. Bucci, Todd A. Clason, and Anthony D. Morielli for their help with DREADDs, and Callum Thomas for his help with microscopy.

Authors report no conflict of interest.

Funding sources: University of Vermont College of Arts and Sciences Seed Grant Award.

Abstract

Operant (instrumental) conditioning is a laboratory analog for voluntary behavior and involves learning to make a response for a reinforcing outcome. The prelimbic cortex (PL), a region of the rodent medial prefrontal cortex, and the dorsomedial striatum (DMS), have been separately established as important in the acquisition of minimally-trained operant behavior. Despite dense anatomical connections between the two regions, experimenters have only recently linked projections from the PL to the posterior DMS in the acquisition of an operant response. Yet, it is still unknown if these projections mediate behavioral expression, and if more anterior regions of the DMS (aDMS), which receive dense projections from the PL, are also involved. Therefore, we utilized designer receptors exclusively activated by designer drugs (DREADDs) to test whether or not projections from the PL to the anterior DMS influence the expression of operant behavior. Rats underwent bilateral PL-targeted infusions of either a DREADD virus (AAV8-hSyn-hM4D(Gi)-mCherry) or a control virus (AAV8-hSyn-GFP). In addition, guide cannulae were implanted bilaterally in the aDMS. Rats were tested with both CNO (DREADD ligand) and vehicle infusions into the aDMS. Animals that had received the DREADD virus, but not the control virus, showed attenuated responding when they received CNO microinfusions into the aDMS, compared to vehicle infusions. Patch clamp electrophysiology verified the inhibitory effect of CNO on DREADDs-expressing PL neurons in acute brain slices. GFP-expressing control PL neurons were unaffected by CNO. The results add to the recent literature suggesting that connections between the PL and aDMS are important for the expression of minimally-trained operant responding.

54 Significance statement

55 Only very recently has it been shown that prelimbic cortex projections to the posterior
56 dorsomedial striatum are important in the acquisition of operant responding. Here, we show that
57 prelimbic cortex projections to the *anterior* dorsomedial striatum are important in the *expression*
58 of operant responding.

59

Chemogenetic silencing of prelimbic cortex to anterior dorsomedial striatum projection attenuates operant responding

Introduction

The prelimbic cortex (PL) has been well established as a mediator of operant (instrumental) responses early in training (Corbit and Balleine, 2003; Killcross and Coutureau, 2003; Ostlund and Balleine, 2005; Tran-Tu-Yen et al., 2009; Trask et al., 2017; Shipman et al., 2018). The dorsomedial striatum (DMS) has similarly been implicated in the acquisition and expression of operant responding, with a particular emphasis on the posterior DMS (pDMS) (Yin et al., 2005a; Yin et al., 2005b; Shiflett et al., 2010). Because the PL and pDMS have both been implicated in the early acquisition of operant responding, it has been suggested that they may function together as part of a greater circuit supporting goal-directed operant responding (Corbit, 2018). Indeed, pharmacological disconnection of these two regions prior to acquisition sessions disrupts the expression of operant responding at test (Hart et al., 2018a).

Traditional disconnection studies do not address the question of whether or not function is mediated by a direct vs. an indirect connection between two brain regions. Recent research using Designer Receptors Exclusively Activated by Designer Drugs (DREADDs) has shown that PL to pDMS projections are important for the acquisition of operant responding (Hart et al., 2018b). Hart, Balleine, and colleagues utilized a dual-virus approach to inactivate the PL-pDMS pathway by infusing AAV-Cre recombinase into the pDMS, and a Cre-dependent DREADDs viral construct into the PL. They found that silencing the PL-pDMS pathway during acquisition, via systemic injection of the DREADDs ligand clozapine-N-oxide (CNO), reduced operant responding during test (Hart et al., 2018b).

The PL has been implicated in the expression of minimally-trained operant responding when testing occurs in the acquisition context (Trask et al., 2017; Shipman et al., 2018). Temporary inactivation of the PL with baclofen/muscimol at the time of test following six daily sessions of acquisition (lever press training) resulted in an attenuation of operant responding in the context where training had been conducted, but not in another context (Trask et al., 2017). Hart et al. (2018) showed that PL projections to posterior DMS are important in the acquisition of operant behavior, but they did not examine whether PL projections to the DMS are important for the expression of operant behavior. In addition, Hart et al. did not examine the function of PL projections to the anterior DMS (aDMS); some studies suggest that PL projections to the anterior DMS (aDMS) are at least as dense as PL projections to pDMS (Mailly et al., 2013; Hunnicut et al., 2016).

In the current experiment, we hypothesized that PL projections to the anterior DMS are involved in the expression of operant responding in the acquisition context. Six weeks prior to training, we infused an AAV8-DREADDs or control viral construct bilaterally into the PL and implanted bilateral guide cannulae into the aDMS. Rats underwent six days of instrumental conditioning followed by infusion of CNO or vehicle into the anterior DMS prior to test. We found that silencing projections from the PL to a relatively anterior region of the DMS attenuated lever-press responding, implicating this pathway in the expression of operant responding. Patch-clamp electrophysiology in a separate group of rats confirmed that CNO suppressed spiking in DREADDs-expressing, layer 5 PL pyramidal neurons but not in PL neurons that expressed the control, GFP, construct.

Methods

"All animal procedures were performed in accordance with the [Author University] animal care committee's regulations."

Subjects

The subjects were 24 male Wistar rats from Charles River Laboratories (St. Constance, Quebec). Rats were 59-63 days old and initially housed in pairs upon arrival. They were given at least 3 days to acclimate to the colony before undergoing surgery. Following surgery, rats were housed individually in a room maintained on a 12:12-h light: dark cycle. Experimentation occurred during the light portion of the cycle.

Surgery

Rats were anaesthetized with isoflurane. pAAV8-hSyn-hM4D(Gi)-mCherry viral construct (gift from Bryan Roth; Addgene plasmid # 50475 ; http://n2t.net/addgene:50475 ; RRID:Addgene_50475) or the control pAAV8-hSyn-EGFP viral construct (gift from Bryan Roth; Addgene plasmid # 50465 ; http://n2t.net/addgene:50465 ; RRID:Addgene_50465) was infused bilaterally into the PL with a Hamilton syringe (stereotaxic coordinates AP: +3.0, ML: +/-0.75, DV: -4.0) at a rate of 0.1µl/min. Each side received an infusion of 0.8µl. The needle was in place for two minutes prior to the start of the infusion to allow the brain to settle, and 10 minutes following completion of the infusion to allow for diffusion away from the needle tip. Guide cannulae (22 gauge, Plastics One) were targeted bilaterally to the anterior DMS at stereotaxic coordinates AP: +1.0, ML:+/-2.0, DV: -3.6. Rats were given carprofen (5.0 mg/kg) for analgesia, as well as bupivacaine around the scalp incision, and Ringer's solution (1.0ml) following surgery. A second dose of carprofen was administered the following day. Rats were

126 weighed and reduced to 90% free feeding weight four days prior to magazine training, and were
127 maintained at 90% free feeding weight throughout the experiment.

128 Apparatus

129 Two sets of four operant chambers were utilized for this experiment (Med Associates
130 model ENV-008-VP, St. Albans, VT). The sets were separated by room and differed slightly in
131 their features. Differentiation of contexts was not required for this experiment, but rats were
132 counterbalanced on vector type and the contexts where they received training/testing. Operant
133 chambers measured 30.5 x 24.1 x 21.0 cm (l x w x h) and the food cup (measuring 5.1 x 5.1 cm)
134 was located within the center of the front wall at a height of 2.5 cm above the floor. All
135 chambers also featured a lever to the left of the magazine (Med Associates model ENV-112CM)
136 that was inserted following a time-out period of two minutes at the beginning of each session.
137 Within each room, each of the four chambers was housed in a sound attenuation chamber. Each
138 chamber was lit by a single incandescent bulb (7.5 W) located on the sound attenuation chamber
139 ceiling. Ventilation fans provided white noise (65 dBA).

140 Half the operant chambers featured clear, acrylic plastic on the walls and a ceiling with
141 brushed aluminum on the front and rear walls. Floor panels were stainless steel grids (0.48 cm
142 diameter) that were staggered so that every other bar was in the opposite of two planes from the
143 previous bar (one plane was 0.5 cm above the other). The other half of the chambers had all floor
144 grids mounted in the same plane with each bar spaced 1.6 cm from the previous bar. The walls in
145 these boxes were also acrylic plastic but featured black, diagonal stripes that were 3.8 cm wide
146 and 3.8 cm apart.

The reinforcer utilized for this experiment was a 45-mg sucrose pellet (5-TUT:1811251, TestDiet, Richmond, IN). The pellet was delivered to the magazine by instruction through a computer located in an adjacent room.

Procedure

All behavioral procedures were conducted so that both tests occurred 6-7 weeks following vector infusion. Rats were run in cohorts of 4 or 8 and counterbalanced across conditions.

Magazine training

All rats received one half-hour session of magazine training. Once all animals were placed in their respective operant chambers, a two-minute time-out period began. During this period, no reinforcers were available. Following that, sucrose reinforcers were freely delivered to the food magazine on a RT 30 schedule. No levers were present during this training.

Acquisition training

Rats then received six daily acquisition sessions. At the start of each session, once all rats were in their respective operant chambers, left levers were inserted into boxes after two min and rats were reinforced on a VI-30 schedule for lever presses. Levers retracted following completion of the half hour session. If rats initially failed to eat sucrose pellets, levers were baited with mashed pellets. One rat had to be removed from further analysis because it failed to eat any pellets and thus failed to acquire the operant lever-pressing response.

Test

After acquisition, all rats underwent two test sessions, separated by a day of retraining. Prior to the first test session, half the rats received a 0.5 µl bilateral intracranial infusion of CNO (1.0 mM) and the other half received a vehicle infusion (artificial CSF (ACSF)) into the DMS (see slice preparation section for more specifics about ACSF composition). The CNO concentration of 1 mM was based on previous studies (Mahler et al., 2014; Lichtenberg et al., 2017). For infusions, dummy cannulae were removed and internal cannulae were inserted into guide cannulae. Internal cannulae tips protruded 1 mm below the tip of guide cannulae. Infusions were delivered over 2 minutes (0.25 µl/minute) by internal cannulae attached to tubing (Intramedic) that connected to Hamilton syringes driven by a microinfusion pump (Kd Scientific). Internal cannulae were allowed to remain in place for one minute following infusions before removal and reinsertion of dummy cannulae. Rats were then placed in transport containers and put into operant chambers 5-15 min after the infusion. After a 2-min period, levers were inserted into the operant chambers (as usual). The test ran for 10 min; lever press responses had no scheduled consequences (i.e., the test was conducted in extinction). The following day, rats received a session of retraining with the VI-30 reinforcement schedule. A second test was given the day after, in which rats received the opposite infusion of the first test. Other than receiving the opposite infusate, testing proceeded exactly as on the first test day.

Histology

Following the second test, rats were injected with a lethal dose of sodium pentobarbital (150 mg/kg, i.p.) and transcardially perfused with phosphate-buffered saline (PBS) followed by 4% paraformaldehyde. Brains were removed and postfixed for one hour before being transferred to a 30% sucrose/PBS solution. After sinking, brains were embedded in OCT and flash-frozen in 2-methyl butane that had been cooled with dry ice. The PL and DMS of each brain were

sectioned at 60µm and floated in phosphate buffer onto slides. Sections were dried in the dark before being mounted with Vectashield mounting medium with DAPI and coverslipped. Viral transfection was examined using a confocal microscope (Nikon C-2) (see representative images in Figures 2 and 3). Excitation lasers were 405 nm (DAPI), 488 nm (EGFP) and 561 nm (mCherry). Viral expression was examined for accuracy by comparing the location of PL cell expression to the PL location in a rat brain atlas (Paxinos and Watson, 2014). Axon terminals were examined for expression directly underneath the deepest part of the cannulae, which were confirmed to be in the DMS.

Slice Preparation for Electrophysiology

Adult Wistar rats, of the same age and from the same supplier as above, were used for patch clamp electrophysiology. Rats underwent PL infusion of viral construct AAV8-hSyn-hM4D(Gi)-mCherry or AAV8-hSyn-EGFP as described above. Following at least six weeks of recovery, electrophysiology experiments were performed. On the experimental day, rats were deeply anesthetized with sodium pentobarbital and transcardially perfused with cold, sucrose-replaced artificial cerebrospinal fluid. The brain was then quickly removed and sliced in the coronal plane on a Leica VT1000S (Leica Instruments) vibratome. Brain slices were then allowed to recover in warmed sucrose-replaced artificial cerebrospinal fluid at 32° C for 30 minutes, and then equilibrated in room temperature artificial cerebrospinal fluid (ACSF) for at least 30 minutes prior to recording. ACSF was composed of the following in mM: NaCl (124), KCl (2.8), CaCl (2), NaH_2PO_4 (1.25), Glucose (10), Sodium Ascorbate (0.4), Sodium Pyruvate (2), $MgSO_4$ (2), and $NaHCO_3$ (26). Sucrose-replaced ACSF was similar to recording-ACSF with the following exceptions in mM: NaCl (0), Sucrose (206), CaCl (1), MgCl (1). Each was pH adjusted to 7.3-7.4 with HCl and osmolarity was 310 ±5 mOsM.

213 Recording Procedures

214 Slices were transferred to a recording chamber (Warner Instruments) and continuously
215 perfused with oxygenated, 32° C ACSF at a rate of 3-4 ml/minute. Virally-infected cells were
216 identified under fluorescent illumination in layer 5 of the PL (Figures 5B and 5D) using a Leica
217 DM-LFSA microscope and Rolera Bolt 3000 CCD camera. Cells were then patched under
218 brightfield/infrared illumination in current clamp mode. Electrodes were made from thin-walled
219 borosilicate glass capillaries (World Precision Instruments) and pulled on a Sutter P-97
220 micropipette puller and filled with a K-glu intracellular solution composed of the following in
221 mM: potassium gluconate (140), KCl (2), MgCl (3), HEPES (10), Phosphocreatine (5), K-ATP
222 (2), Na-GTP (0.2) and pH adjusted to 7.3-7.4. Cells were clamped with a Multiclamp 700B
223 controller and Multiclamp software (Molecular Devices). Data from patched cells was acquired
224 using a Digidata 1440 interface (Molecular Devices) and pClamp software (Molecular Devices).
225 Patched neurons equilibrated for approximately 5 minutes following successful whole cell
226 configuration. Access resistance was monitored throughout experiments and if it reached above
227 25 MΩ, or changed by > 20%, recordings were discarded. Patched neurons were considered
228 acceptably healthy with a resting membrane potential below -50 mV and an action potential
229 overshoot greater than +10 mV. Excitability curves were generated by injecting progressively
230 larger positive current at 50 pA increments from 0-450 pA at the highest level of stimulation and
231 counting the number of spikes at each level. This was done prior to CNO exposure, and after 4-6
232 minutes of 10 μM CNO exposure. Spike curves were analyzed using Clampfit software
233 (Molecular Devices).

234 Statistical analysis

IBM SPSS 25.0 was used for data analysis. A repeated measures ANOVA was used to examine responses per minute across acquisition sessions and test sessions. The rejection criterion was set at $p<0.05$. Following a significant interaction, within-subjects comparisons (two-tailed paired-samples t-tests) were performed to determine the source of the interaction. Effect size was calculated as Cohen's d for all significant effects (see Table 1) (Cohen, 1988; Rosenthal, 1994).

Results

Four rats (2 DREADD, 2 GFP) were removed prior to analysis: one rat did not acquire the lever-press response, two rats had a viral vector infusion site dorsal to the PL, and one rat had extensive cannula-related damage to the DMS (see further explanation in histology section). This left 10 rats in each group.

Acquisition

All rats increased responding (lever presses/minute) across training sessions, indicating successful learning of the operant response (see Figure 1A). A 2 (Vector: DREADD vs GFP) x 6 (session) repeated-measures ANOVA yielded a main effect of session, F (5,90)= 56.18, MSE= 9.78, $p<.001$[a], but no main effect of vector or a vector x session interaction (F's<1).

Test

Inactivation of the PL-anterior DMS pathway attenuated the expression of operant responding during the test (see Figure 1B). A 2 (Vector: DREADD vs GFP) x 2 (Drug: CNO vs vehicle) repeated-measures ANOVA yielded a significant vector x drug interaction, F (1,18)= 5.08, MSE= 1.95, $p= 0.04$[b]. Follow-up paired-samples t-tests compared lever-press responding after CNO vs vehicle for each vector group separately. The DREADD group showed an

attenuation of responding when tested with a CNO infusion, t (9)= 2.36, p= 0.04[c]. In contrast, the rats that had received the GFP vector showed no difference in responding following CNO vs vehicle infusions into the DMS, t (9)= 1.31, p= 0.22[d]. The pattern indicates that intra-DMS CNO effects were selective to the rats that had received PL DREADD transfection.

Histology

DREADD-mCherry expression and control GFP expression were verified in the cell bodies of the PL and axon terminals of the DMS in all rats. Examples are shown in Figure 2. Examples are also shown of typical dorsal-ventral and posterior-most spread from the PL infusion site (Figure 3). Two rats were removed because the viral-vector infusion site in the PL was too shallow. Cannula placements in the DMS were also verified (Figure 4). No rats had to be excluded from analysis for incorrect cannula placement, though one brain showed extensive damage from a cannula (possibly from infection) that affected tissue well beyond the cannula tract and DMS. This rat was excluded from analysis. Thus, three rats were removed during verification of viral expression, leaving the DREADD group with a final n of 10 and the GFP group with a final n of 10.

Electrophysiology

To confirm the effect of CNO on DREADDs-expressing PL pyramidal neurons, we used whole-cell patch-clamp electrophysiology to compare spike activity (number of spikes to 10 current steps, 0-450 pA) before and after CNO exposure (see Figure 5). DREADDs-expressing PL neurons showed fewer spikes than non-expressing neurons after CNO exposure. In contrast, non-DREADDs expressing PL neurons spiked slightly more after CNO exposure, possibly because of CNO suppression of nearby DREADDs-expressing inhibitory interneurons.

A 2 (Drug: CNO vs vehicle) x 10 (Current: 0-450 pA) repeated-measures ANOVA on DREADDs-expressing PL neurons revealed a significant main effect of CNO on neuron spiking, F (1, 4)= 7.83, MSE= 31.49, p= 0.049[e], and a significant drug x current interaction, F (9, 36)= 4.52, MSE= 2.82, p= 0.001[e]. Follow-up paired-samples t-tests comparing CNO vs. vehicle at each current step revealed significantly fewer spikes with CNO at current steps of 200-, 250-, and 300-pA (p's < 0.046[f]) (see Figure 5A). The same analyses on GFP-expressing PL neurons revealed no CNO or drug x current interaction effects, p's > 0.45 (see Figure 5C).

Discussion

The present results suggest that PL projections to a relatively anterior region of the DMS are involved in the expression of operant responding. This finding expands upon the work by Trask et al. (2017) that had found involvement of the PL in expression of operant responding in the same paradigm, as well as that of Hart et al. (2018), who demonstrated a role for PL-to-*posterior* DMS projections in the *acquisition* of goal-directed operant responding. The current results contrastingly show that a PL-to-a more *anterior* DMS pathway is important in the *expression* of operant responding early in training. This is unlikely to be a motor-related effect, given that studies have demonstrated that pharmacological inactivation of the PL (and therefore all of its projections) reduces only minimally-trained responding, and only in the acquisition context, while leaving other responses unaffected (Killcross and Coutureau, 2003; Trask et al., 2017; Shipman et al., 2018). Finally, we confirmed with *ex vivo* patch-clamp electrophysiology that cells in layer 5 of the PL expressing the DREADD-mCherry construct reporter showed attenuated spiking in the presence of CNO. Spiking of PL neurons expressing only the control GFP reporter was unaffected by CNO.

Though statistically significant, the size of the reduction in responding was numerically small in our DREADDs-expressing rats. However, there are several important points to keep in mind. First, we inactivated only a subset of projections from the PL to the aDMS, and the inactivation was probably less than total, as suggested by our electrophysiology results. Second, it is likely that other PL projections, besides just those to the aDMS, are important in expression of minimally-trained operating responding in the acquisition context; indeed, others (Trask et al., 2017) have shown a fairly large attenuation of responding with pharmacological inactivation of PL, which would inactivate all PL projections. Finally, it is worth comparing the magnitude of our effects to those of Hart et al., (2018), who used a dual-vector approach and intraperitoneal injections of CNO during acquisition to silence PL-pDMS projections. Hart et al. (2018) reported that in a 5-min choice (still-valued R2 vs. devalued R1) test session, DREADDs-expressing rats that had received vehicle injection prior to acquisition sessions emitted an average of approximately 18 R2 lever-presses; a separate group of DREADDs-expressing rats that had received CNO injection prior to acquisition sessions emitted an average of approximately 12 R2 lever-presses. This translates to a reduction of approximately 1 lever-press per min. We found that during a 10-min test session, vehicle-infused DREADDs-expressing rats emitted an average of approximately 86 responses while CNO-infused DREADDs-expressing rats emitted an average of approximately 76 responses. This also translates to a reduction of 1 lever-press per min. Thus, despite a difference in methods and DMS terminal locations, the magnitude of operant response reduction as a result of DREADDs-mediated inactivation of PL-DMS terminals was similar in Hart et al. (2018) and our experiment.

A recent concern with the use of DREADDs is that CNO does not appear to cross the blood-brain barrier; instead, the effects of systemic injections of CNO may be via the CNO

metabolite clozapine, which binds with high affinity to DREADDs and binds with endogenous receptors (Gomez et al., 2017). We avoided this issue here by using intracranial CNO infusions. However, there may still be off-target effects caused by the use of a relatively high concentration of CNO in this method (Gomez et al., 2017). Therefore, we included two control procedures: (1) a group of rats that did not express DREADDs and (2) all rats received CNO and vehicle, in separate tests. Thus, we controlled for CNO effects as well as for potential vector effects. We also note here that an additional caveat to circuit-specific manipulation using DREADDs is that it may be difficult to completely isolate a specific pathway. For example, collateral projections of projection neurons expressing DREADDs may also be activated/inactivated by CNO. However, it is unclear how likely this is given that CNO is infused directly into the DMS.

We verified that CNO reduced spiking in PL neurons expressing DREADDs-mCherry while having no effect on spiking in PL neurons expressing GFP. However, this leaves unaddressed the question of whether or not CNO reduced spiking in DMS neurons as a result of reducing spiking in PL neurons projecting to the DMS. It seems likely that it did: first, the most straightforward interpretation of our behavioral results is that intra-DMS CNO reduced activation of PL projections to the DMS, which in turn reduced DMS activation. It is unlikely that CNO affected DMS neurons directly, since rats that did not express DREADDs were unaffected by intra-DMS CNO. Second, Lichtenberg et al. (2017) co-expressed the same DREADDs-mCherry construct as we used, along with channelrhodopsin, in neurons in the orbitofrontal cortex (OFC) and patch-clamped neurons in the basolateral amygdala (BLA) that were nearby fluorescing OFC terminals. Excitatory post-synaptic currents in these BLA neurons, produced by optical activation of fluorescing OFC terminals, were reduced in the presence of CNO. This suggests that CNO does reduce axon terminal activity in this DREADDs-mCherry

construct. In addition, the design of our behavioral experiment makes alternative explanations less likely.

Like Hart et al. (2018), we examined a role for PL-to-DMS projections in minimally trained operant responding, though our methods differ on a few critical points. First, we only trained one response with one outcome. Hart et al. trained two lever-press responses, each with its own unique outcome, and both levers were available during (choice) testing. Second, we did not devalue our reinforcer; thus we did not distinguish between goal-directed vs. habitual behavior. Third, we examined the PL-DMS pathway in a more anterior portion of the DMS (e.g., guide cannula implanted at +1.0 mm AP from bregma in our study vs. AAV-Cre infusion at -0.4 to -0.5 mm AP in Hart et al., 2018b), rather than the PL projections to posterior DMS regions that have been more frequently associated with acquisition of goal-directed behavior. Fourth, we examined expression of responding, rather than the acquisition of responding, by inactivating the PL-DMS pathway prior to test rather than prior to each acquisition session. Finally, we utilized a different means of pathway-specific chemogenetic inactivation, implanting cannulae into the DMS to inactivate PL axon terminals after AAV8-DREADD infusion into the PL. In contrast, Hart et al. utilized a dual-virus approach, infusing a Cre-dependent DREADD viral construct into the PL and a Cre recombinase viral construct into the pDMS, and then inactivating the PL-pDMS pathway with intraperitoneal injection of CNO. Overall, our findings complement those of Hart et al. (2018) who showed that the PL-pDMS pathway is important for the acquisition of goal-directed behavior. We show here that the PL-aDMS pathway is important for expression of minimally-trained operant behavior.

Many of the studies investigating the role of the PL in operant behavior have additionally confirmed whether responding was goal-directed or habitual (Corbit and Balleine, 2003;

Killcross and Coutureau, 2003; Ostlund and Balleine, 2005; Tran-Tu-Yen et al., 2009; Shipman et al., 2018). Behavior is considered goal-directed if it is sensitive to reinforcer devaluation, whereas habitual behavior is insensitive to reinforcer devaluation. Though we did not utilize reinforcer devaluation to examine if our behavior was goal-directed, it is reasonable to assume that our minimally-trained operant response was goal-directed, as habit typically develops across many training sessions (Dickinson, 1985). This is further supported by the findings of Shipman et al. (2018), who showed that the PL plays a transitory role in the development of operant responding: inactivation of PL reduced minimally-trained goal-directed instrumental behavior, but not more extensively-trained instrumental behavior that is goal-directed. The PL has never been linked to habit.

Despite dense anatomical connections from the PL to the aDMS, research has tended to focus on the pDMS in goal-directed behavior. The pDMS has been defined as the DMS beginning around +0.24 mm anterior to bregma (Hart and Balleine, 2017). The focus on the pDMS is largely based on an early study by Yin and colleagues (Yin et al., 2005b). Yin et al. (2005) found that pre-training or post-training lesions of the posterior region of the DMS impaired the acquisition and expression of goal-directed behavior (target posterior coordinates at -0.4 mm AP relative to bregma, compared to +1.0 mm AP in the current study). However, the effects of aDMS lesions were actually somewhat inconclusive, as pre-training aDMS lesions did not affect expression of goal-directed behavior at test but post-training aDMS lesions did. Other research has provided support for the idea that the pDMS, but not the aDMS, is important for goal-directed responding. For example, functional disconnection of the parafascicular thalamus and pDMS disrupts goal-directed responding, whereas disconnection of the parafascicular thalamus and aDMS has no effect (Bradfield et al., 2013).

Nonetheless, other studies have found that the aDMS, in addition to the pDMS, is important for goal-directed behavior. Corbit and Janak (2010) trained two different lever-press responses and then used satiation to devalue the outcome associated with one response. They found that temporary inactivation with baclofen/muscimol of either the anterior DMS or posterior DMS (coordinates at +1.2 mm and -0.3 mm AP relative to bregma, respectively) during acquisition resulted in insensitivity to outcome devaluation at time of test in an operant task (Corbit and Janak, 2010). This result suggests that aDMS and pDMS both seem to be involved in goal-directed responding. Further studies by this lab also showed a role for the anterior DMS in goal-directed behavior with an alcohol reinforcer (Corbit et al., 2012). Thus, there is some evidence for aDMS involvement in goal-directed behavior despite a literature that focuses largely on the pDMS.

In conclusion, we found that the PL-aDMS pathway is important in the expression of operant responding. Thus, we expand upon previous research to show, using circuit-specific chemogenetic silencing, a role for a PL-to-anterior DMS pathway in the expression of operant behavior to complement the demonstrated role of a PL-to-posterior DMS pathway in the acquisition of operant behavior.

410 References

411 Bradfield LA, Bertran-Gonzalez J, Chieng B, Balleine BW (2013) Thalamostriatal pathway and
412 cholinergic control of goal-directed action: Interlacing new with existing learning in the
413 striatum. Neuron 79:153-166.
414 Cohen J (1988) Statistical Power Analysis for the Behavioral Sciences, 2nd Edition. Hillsdale,
415 NJ: Erlbaum.
416 Corbit LH (2018) Understanding the balance between goal-directed and habitual behavioral
417 control. Current Opinion in Behavioral Sciences 20:161-168.
418 Corbit LH, Balleine BW (2003) The role of the prelimbic cortex in instrumental conditioning.
419 Behavioural Brain Research 146:145-157.
420 Corbit LH, Janak PH (2010) Posterior dorsomedial striatum is critical for both selective
421 instrumental and Pavlovian reward learning. European Journal of Neuroscience 31:1312-
422 1321.
423 Corbit LH, Nie H, Janak PH (2012) Habitual alcohol seeking: Time course and the contribution
424 of subregions of the dorsal striatum. Biological Psychiatry 72:389-395.
425 Dickinson A (1985) Actions and habits: The development of behavioural autonomy.
426 Philosophical Transactions of the Royal Society B: Biological Sciences 308:67-78.
427 Gomez JL, Bonaventura J, Lesniak W, Mathews WB, Sysa-Shah P, Rodriguez LA, Ellis RJ,
428 Richie CT, Harvey BK, Dannals RF, Pomper MG, Bonci A, Michaelides M (2017)
429 Chemogenetics revealed: DREADD occupancy and activation via converted clozapine.
430 Science 357:503-507.
431 Hart G, Balleine BW (2017) Medial striatum. In: Encyclopedia of Animal Cognition and
432 Behavior (Vonk J, Shackelford, eds). Basel, Switzerland: Springer International
433 Publishing.
434 Hart G, Bradfield LA, Balleine BW (2018a) Prefrontal cortico-striatal disconnection blocks the
435 acquisition of goal-directed action. Journal of Neuroscience 38:1311-1322.
436 Hart G, Bradfield LA, Fok SY, Chieng B, Balleine BW (2018b) The bilateral prefronto-striatal
437 pathway is necessary for learning new goal-directed actions. Curr Biol 28:1-12.
438 Hunnicut BJ, Jongbloets BC, Birdsong WT, Gertz KJ, Zhong H, Mao T (2016) A comprehensive
439 excitatory input map of the striatum reveals novel functional organization. eLife
440 5:e19103.
441 Killcross S, Coutureau E (2003) Coordination of actions and habits in the medial prefrontal
442 cortex of rats. Cerebral Cortex 13:400-408.
443 Lichtenberg NT, Pennington ZT, Holley SM, Greenfield VY, Cepeda C, Levine MS, Wassum
444 KM (2017) Basolateral amygdala to orbitofrontal cortex projections enable cue-triggered
445 reward expectations. Journal of Neuroscience 37:8374-8384.
446 Mahler SV, Vazey EM, Beckley JT, Keistler CR, McGlinchey EM, Kaufling J, Wilson SP,
447 Deisseroth K, Woodward JJ, Aston-Jones G (2014) Designer receptors show role for
448 ventral pallidum input to ventral tegmental area in cocaine seeking. Nat Neurosci 17:577-
449 585.
450 Mailly P, Aliane V, Groenwegen HJ, Haber SN, Deniau J-M (2013) The rat prefrontalstriatal
451 system analyzed in 3D: Evidence for multiple interacting functional units. Journal of
452 Neuroscience 33:5718-5727.
453 Ostlund SB, Balleine BW (2005) Lesions of the medial prefrontal cortex disrupt the acquisition
454 but not the expression of goal-directed learning. Journal of Neuroscience 25:7763-7770.

Paxinos G, Watson C (2014) The Rat Brain in Stereotaxic Coordinates, 7th Edition. London, UK: Academic Press.

Rosenthal R (1994) Parametric measures of effect size. In: The Handbook of Research Synthesis (Cooper H, Hedges LV, eds). New York, NY: Sage.

Shiflett MW, Brown RA, Balleine BW (2010) Acquisition and performance of goal-directed instrumental actions depends on ERK signaling in distinct regions of dorsal striatum in rats. Journal of Neuroscience 30:2951-2959.

Shipman ML, Trask S, Bouton ME, Green JT (2018) Inactivation of prelimbic and infralimbic cortex respectively affects minimally-trained and extensively-trained goal-directed actions. Neurobiology of Learning and Memory 155:164-172.

Tran-Tu-Yen DAS, Marchand AR, Pape J-R, DiScala G, Coutureau E (2009) Transient role of the rat prelimbic cortex in goal-directed behaviour. European Journal of Neuroscience 30:464-471.

Trask S, Shipman ML, Green JT, Bouton ME (2017) Inactivation of the prelimbic cortex attenuates context-dependent operant responding. Journal of Neuroscience 37:2317-2324.

Yin HH, Knowlton BJ, Balleine BW (2005a) Blockade of NMDA receptors in the dorsomedial striatum prevents action-outcome learning in instrumental conditioning. European Journal of Neuroscience 22:505-512.

Yin HH, Ostlund SB, Knowlton BJ, Balleine BW (2005b) The role of the dorsomedial striatum in instrumental conditioning. European Journal of Neuroscience 22:513-523.

492 Table 1. Data structure, type of test used to analyze the data, and observed power of key results.

	Data Structure	Type of test	Power (Cohen's d)
a	Normal distribution	Repeated Measures ANOVA	Main effect Session: 1.784
b	Normal distribution	Repeated Measures ANOVA	Interaction (Drug x Vector): 0.247
c	Normal distribution	Paired Samples *T* test	Main effect Drug: 0.745
d	Normal distribution	Paired Samples *T* test	Not significant
e	Normal distribution	Repeated Measures ANOVA	Main effect CNO: 0.388 Interaction (Drug x Current): 0.262
f	Normal distribution	Paired samples *T* tests	Main effects Current: 200 pA: 1.204 250 pA: 3.095 300 pA: 2.807

493
494
495
496
497
498

Figure 1: A. Acquisition of lever-press response over six training sessions with one retraining session in between the two test sessions. Mean ± SEM. B. Test session results for rats that had received the DREADD or control (GFP) construct in the prelimbic cortex. CNO or vehicle was infused into the aDMS prior to the first test session, and rats received the opposite infusate prior to the second test session. Order of infusion was counterbalanced in each group. * = $p<0.05$.

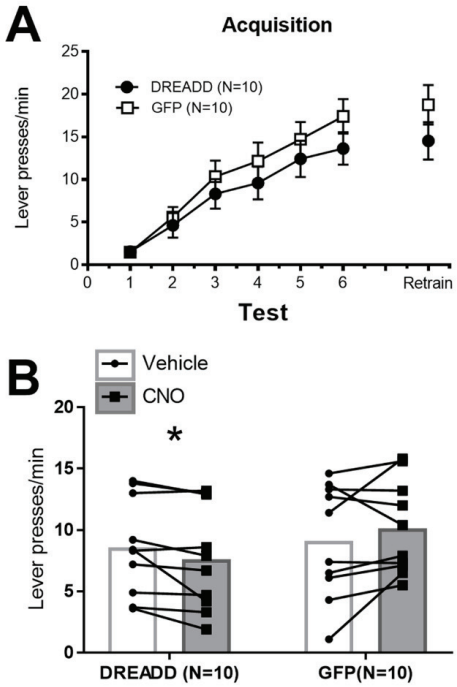

Figure 2. A. Location (left panel) and representative images (right panels) of cell bodies expressing DREADDs-mCherry construct (left) or GFP control construct (right) in the PL (area 32) at 40x. Blue is DAPI nuclear stain. B. Location (left panel) and representative images (right panels) of axon terminals in anterior DMS expressing DREADDs-mCherry (left) or GFP (right) at 60x. Scale bars are 50 µm.

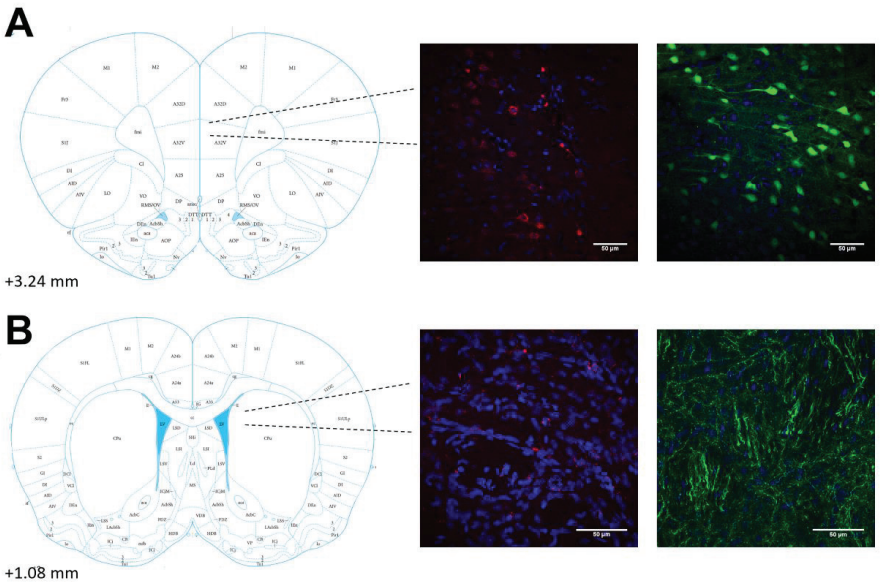

Figure 3: Location and representative DREADDs-mCherry (A) and GFP (B) spread in the prelimbic cortex (area 32) at 20x. Top panels are the infusion site and bottom panels are estimated posterior-most spread. Stitching was done with a 3% overlap in the images and each frame within the final image was 2048 x 2048 pixels. Scale bars = 100 µm.

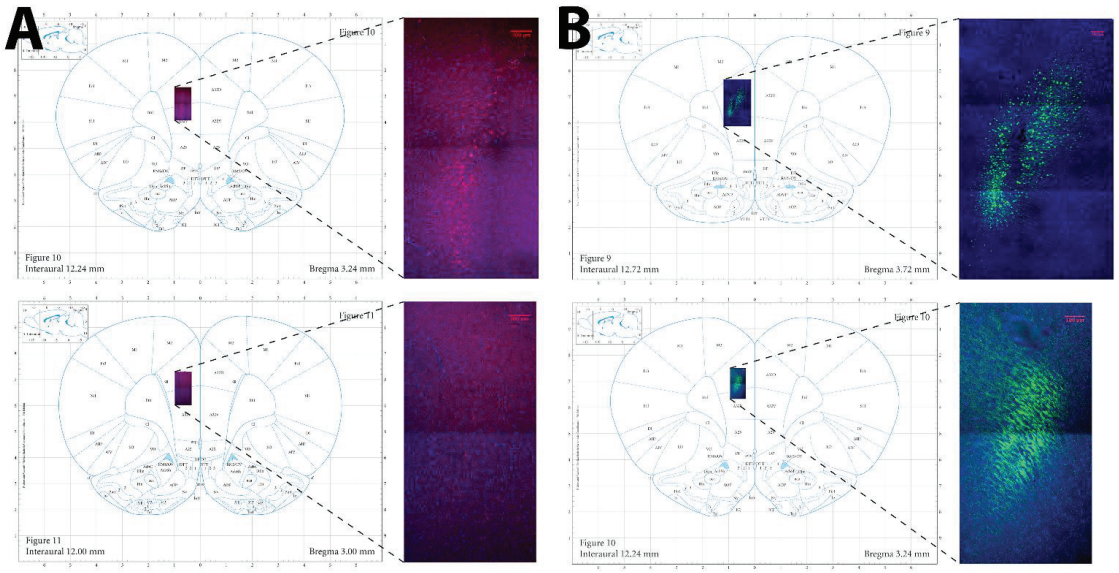

Figure 4. Left panel. Infusion sites in anterior DMS. Numbers are anterior-posterior distance in mm from bregma. Right panel. Example cannula placement. Shown is the right hemisphere. CN = guide cannula track. Guide cannula tips were above the DMS. The thin white bar shows where the infusion cannula (which protruded 1 mm below the tip of the guide cannula) was. STR = striatum. LV = lateral ventricle. Scale bar = 500 µm.

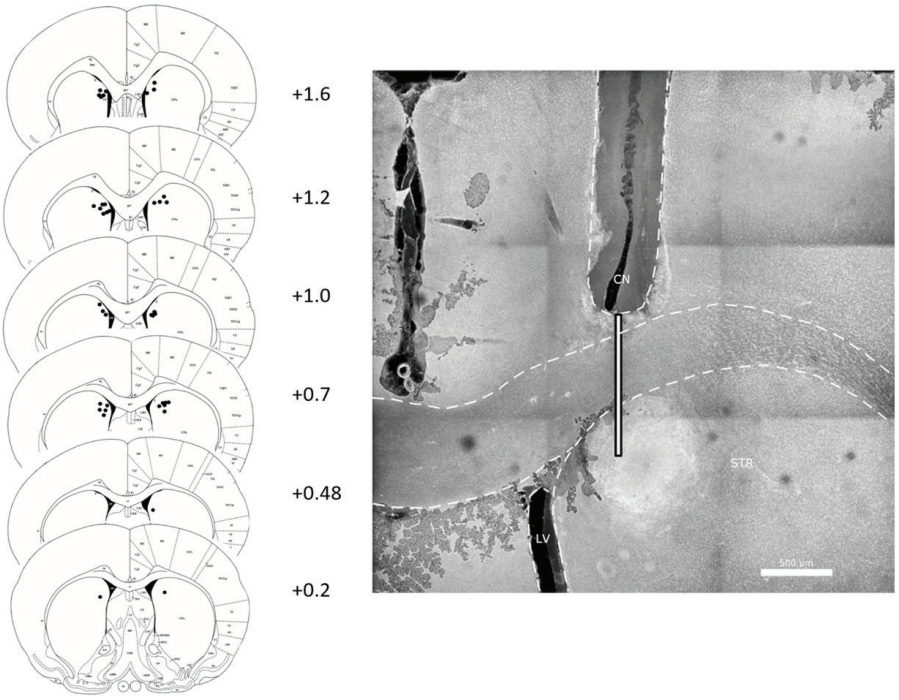

Figure 5: A. Excitability curve shows spikes elicited to progressively larger current injection of DREADDs-mCherry-expressing PL pyramidal cells before and after CNO (10 µM) exposure. B. Example image of DREADDs-mCherry-expressing PL pyramidal cell in fluorescent (left), and infrared (right). C. Excitability curve shows spikes elicited to progressively larger current injection of GFP-expressing PL pyramidal cells before and after CNO (10 µM) exposure. B. Example image of GFP-expressing PL pyramidal cell in fluorescent (left), and infrared (right). E. Example trace of DREADDs-expressing PL neuron; 4 minutes of CNO exposure caused a reduction in spike frequency to current injection compared to baseline, while removal of CNO from the bath caused a partial recovery of spike frequency. Scale bars are 20 mV and 100 ms, and stimulation was 250 pA and 350 pA for 1 second.